Physica A 388 (2009) 3233–3243

Contents lists available at ScienceDirect

Physica A

journal homepage: www.elsevier.com/locate/physa

Discontinuous transition from free flow to synchronized flow induced by short-range interaction between vehicles in a three-phase traffic flow model

Kun Gao [a,*], Rui Jiang [b], Bing-Hong Wang [a], Qing-Song Wu [b]

[a] Department of Modern Physics, University of Science and Technology of China, Hefei, Anhui, 230026, PR China
[b] School of Engineering Science, University of Science and Technology of China, Hefei, Anhui, 230026, PR China

ARTICLE INFO

Article history:
Received 2 January 2009
Received in revised form 12 April 2009
Available online 3 May 2009

PACS:
45.70.Vn
05.40.-a
02.60.Cb
05.65.+b

Keywords:
Three-phase traffic flow
Breakdown phenomenon
Synchronized flow
Fundamental diagram

ABSTRACT

In this paper, we incorporate a limitation on the interaction range between neighboring vehicles into the cellular automaton model proposed by Gao and Jiang et al. [K. Gao, R. Jiang, S. X. Hu, B. H. Wang and Q. S. Wu, Phys. Rev. E 76 (2007) 026105], which was established within the framework of Kerner's three-phase traffic theory and has been shown to be able to reproduce the three-phase traffic flow. This modification eliminates an unrealistic phenomenon found in the previous model, where the velocity-adaptation effect between neighboring vehicles can exist even if those vehicles are infinitely far away from each other. Therefore, in the improved model, we regulate that such interactions can only occur within a finite distance. For simplicity, we suppose a constant value to describe this distance in this paper. As a result, when compared to the previous model, the improved model mainly simulates the following results which are believed to be an improvement. (1) The improved model successfully reproduces the expected discontinuous transition from free flow to synchronized flow and the related "moving synchronized flow pattern", which are both absent in the original model but have been observed in real traffic. (2) The improved model simulates the correlation functions, time headway distributions and optimal velocity functions which are all more consistent with the empirical data than the previous model and most of the other models published before. (3) Together with the previous two models considering the velocity-difference effect, this model finally accomplishes a significative process of developing traffic flow models from the traditional "fundamental diagram approach" to the three-phase traffic theory. This process should be helpful for us to understand the traffic dynamics and mechanics further and deeper.

1. Introduction: Traffic flow theory and traffic flow models

Vehicular traffic has become a title of physics over the last sixty years. Traffic states are often described as some kinds of fluid or flow thus are widely called the "traffic flow". The dynamics of traffic flow can be recognized as some certain evolutionary motions of typical nonlinear complex systems and have attracted much interest from physicists and mathematicians [1–13]. In order to explore the essential rules of the traffic flow, researchers carried out large amounts of traffic measures and observations, and established various types of theoretical or computational models based on the data. Usually, there are many different ways to explore the traffic models, under different theoretical hypothesis. With phase transition thought to exist in traffic flow, the fundamental diagram approach (two-phase hypothesis) and the three-phase traffic theory (three-phase hypothesis) have now become the main branches of the modern traffic flow theories.

* Corresponding author.
E-mail addresses: kgao@mail.ustc.edu.cn (K. Gao), rjiang@ustc.edu.cn (R. Jiang).

0378-4371/$ – see front matter © 2009 Elsevier B.V. All rights reserved.
doi:10.1016/j.physa.2009.04.033

1.1. The fundamental diagram approach

From the 1950s on, several different approaches were developed to simulate the traffic flow, including the macroscopic models (the hydrodynamics models [14–20]), the mesoscopic models (the gas-kinetic models [21–24] and the microscopic models (the car-following models [25,26] and the cellular automaton models [27–30]). Since the phase transition theory was applied on the traffic flow research, most traffic flow models or empirical formulations were established based on a two-phase hypothesis, under which the traffic states can be classified into two different traffic phases, i.e., the free flow (F) phase and the jammed phase (J). These two traffic phases have obvious differences in their spatial-temporal features and can be distinguished by a phase-transition point in the flow-density plane. The flow-density curve, which goes across the original point and has at least one maximum, is often called "the fundamental diagram" of traffic flow. Therefore, traffic theories in this framework are summarized as a "fundamental diagram approach" [2,3,31].

The fundamental diagram approach is quite successful in describing the traffic states and traffic evolutions. It can reproduce important features like the forming and dissolving of queues in the traffic system. So it has been widely accepted and well developed during the past decades. However, the two-phase classification in the fundamental diagram approach implies that there are only two kinds of traffic states, either free flow or jams, could be long-time steady and form a phase. Intermediate states between them, usually shown as low-speed but uninterrupted traffic states, are not yet studied adequately. These states are simply considered as temporary and unsteady states, which are of little importance to the features of the traffic system. Therefore, the fundamental diagram approach studies the traffic flow in a static way. Interactions between vehicles are either vanished (in free flow) or extremely strong (in jams), without any intermediate status. Dynamically equivalent states, which should be very popular in real traffic, are seldom studied in the fundamental diagram approach.

1.2. Kerner's three-phase traffic theory

Based on a fairly long observation of the traffic flow on the German highways A5, A1, A44, and A3 between 1995 and 1998, B.S. Kerner introduced a three-phase traffic theory [32,33], which has been used by Kerner together with his colleagues for the development of some three-phase traffic flow models and methods of traffic engineering [34–43]. Three-phase traffic theory shows us a brand new prospect on the highway traffic systems [32–40,44,45]. It impels forward the previous phase-transition theory in the traffic flow from a two-phase limitation to a possible multi-phase structure. Being different to the traditional "fundamental diagram approach", three-phase traffic theory further distinguished the congested traffic states into wide moving jams and a newly defined state called the "synchronized flow" (S). Synchronized flow can be considered as an intermediate state between the free flow and the wide-moving jams, with middle levels of speeds, densities and fluxes. Being different to the temporary states in the fundamental diagram approach, synchronized flow contains inner fluctuations within a fairly wide amplitude, but the entire phase can be kept long-time steady and nearly homogeneous. It also has its own characteristics thus could possibly be distinguished as an individual phase. As a result, there are totally three different types of traffic states which divide all the possible traffic flow states into three traffic phases, i.e., the free flow (F), the synchronized flow (S) and the wide moving jams (J).

Supposed to be different phases, free flow, synchronized flow and wide moving jams should have distinguishable properties of their own. As we know from the fundamental diagram approach, free flow could be characterized by the weak interactions among vehicles, while wide moving jams could be characterized by the long-time stop of vehicles and extremely strong blocks. In the same way, for synchronized flow, Kerner pointed out that synchronized flow is characterized by a considerably high flux without any clear density-flux relations. The speeds of vehicles, and the distances or interactions between vehicles, are all middle-leveled and quite flexible. Furthermore, Kerner has proposed a fundamental hypothesis of his three-phase traffic theory, which says that the steady states of synchronized flow cover a two-dimensional region in the flow-density plane. Evolutions within the synchronized flow phase are represented as random walks of the data points in the flow-density plane. Synchronized flow usually looks nearly homogeneous in macroscopic scales in the spatial-temporal diagram and can keep steady for quite a long time until a phase transition occurs [32–40,44–48].

As we can see, the definition of the synchronized flow and the phase transitions between the synchronized flow phase and the other two traffic phases would be the kernel of the three-phase traffic theory. In Kerner's hypothesis, all the phase transitions among the three traffic phases are first-order/discontinuous. However, only the phase transition between free flow and synchronized flow ($F \leftrightarrow S$) and the phase transition between synchronized flow and wide moving jams ($S \leftrightarrow J$) can spontaneously occur. Under ceratin scales of vehicle densities, either of these two phase transitions can occur with probabilities, induced by the random fluctuations occurring somewhere in the traffic flow. When the extent of the random fluctuation is higher than a threshold value, the phase transition occurs. The probability of the phase transition will increase with an increase of density or time. On the other hand, the phase transition from free flow to jams ($F \rightarrow S$) can only occur due to some external inducements such as traffic signals or closure of the road.

With these three traffic phases and two phase transitions occurring with probabilities among them, the three-phase traffic theory has provided an instructive viewpoint to understand the traffic dynamics and the empirical findings. In particular, the three-phase traffic theory gives more reasonable descriptions on the bottleneck induced congested patterns than the fundamental diagram approach. It has been discovered from traffic observations that with different sets of flow rates on the main road and the on-ramp, different congested patterns emerge at the upstream of the bottleneck. These

different congested patterns have different spatial-temporal features to each other, which can be qualitatively distinguished easily. Empirical results tell us that the stop and go waves (traffic jams) can only emerge when the on-ramp flow is high enough, namely, under a strong bottleneck; on the other hand, lower on-ramp flow (weak bottleneck) can only induce some kinds of "homogenous congested traffic". In the framework of the three-phase traffic theory, Kerner differentiated the bottleneck-induced congested states into the following six patterns by different scales of the flows: (1) general pattern (GP); (2) widening synchronized flow pattern (WSP), (3) dissolving general pattern (DGP), (4) local synchronized flow pattern (LSP), (5) moving synchronized flow pattern (MSP) and (6) synchronized flow pattern with alternations of free flow and synchronized flow (ASP). Among them, GP occurs under strong bottlenecks. It consists of a synchronized flow region and a series of spontaneously emerged wide moving jams from the original synchronized flow region. While the WSP occurs under weak bottlenecks, consisting of a widening region of synchronized flow which is nearly homogeneous. Therefore, compared to the empirical results, the three-phase traffic theory provides consistent descriptions on these congested patterns. The related empirical evidence has thus provided strong support for the three-phase traffic theory.

However, on the other hand, nearly all the two-phase traffic flow models, which are under the framework of the fundamental diagram approach, give us quite different results. In these results, stop and go waves emerge under weak bottlenecks while homogeneous congested traffic occurs under strong bottlenecks [8,49–51]. Simulation results are contradictory to the empirical results. This becomes an obvious drawback for the validity of the fundamental diagram approach. As a result, the three-phase traffic theory is much better sustained by empirical data and has thus come to be accepted by more researchers.

Furthermore, investigations on single vehicle data have discovered that each of the three traffic phases has a particular microscopic structure; even free flow is not as trivial as previously believed [52]. Therefore, a suitable traffic theory is required not only to describe right traffic phases and phase transitions, but also to present the microscopic structures of the traffic flow properly. These requirements bring forward new challenges to the traffic flow theories and impel researchers to study their theories on microscopic scales.

In this paper, we will show a cellular automaton (CA) model in the framework of the three-phase traffic theory. We are going to show this model is consistent with the empirical data and the hypothesis of the three-phase traffic theory in both macroscopic and microscopic ways.

2. Previous models in the framework of the three-phase traffic theory

So far, there mainly exist three different series of traffic flow models which are consistent with the three-phase traffic theory, i.e., the models by Kerner, Klenov and Wolf [41,42,53,54], the model by Lee [55], and the models by Jiang and Wu [56,57]. These models were designed by considering different aspects of possible vehicular traffic dynamics, and most of them were represented by cellular automaton (CA) modeling approach. In 2007, Gao, Jiang and Hu et al. proposed other possible driving mechanics in their CA traffic flow models [58,59]. These models focus on the influence of the velocity-difference between two successive vehicles on the randomization process of the following one (so that we call them "Velocity-difference effect (VDE)" series models in this paper). This mechanics reflects the fact that drivers usually adapt their acceleration and deceleration motions according to their relative speeds to the vehicles in front of them. When the front vehicle moves faster, the driver will feel confident that a sudden deceleration is unlikely to be required and will feel safer as a result. On the other hand, when the following vehicle moves faster than the front vehicle, the driver will feel nervous and perhaps decelerate as a result of this anxiety. Similar mechanics have ever been described in the classic car-following equations as

$$\frac{\mathrm{d}v_n}{\mathrm{d}t}(t) = \lambda \Delta v_n \tag{1}$$

in which Δv_n is the velocity-difference between neighboring vehicles, and λ is the sensitive parameter.

In the VDE series models, the earliest version was published in Ref. [58] (called VDE-I model). The VDE-I model simply substitutes the constant randomization parameter p in the NS model with a variable depending on the velocity-difference as

$$p = \begin{cases} p_-, & For \quad v_i(t) < v_{i-1}(t) \\ p_0, & For \quad v_i(t) = v_{i-1}(t) \\ p_+, & For \quad v_i(t) > v_{i-1}(t), \end{cases}$$

with all the other regulations of the NS model unchanged at the same time. This model executes the driving mechanics mentioned above by changing the randomization probability of the following vehicle. As a result, it produces some special states which are similar in certain aspects to the synchronized flow. In more detail, these states have quite similar spatial-temporal features to the synchronized flow, but can't show proper phase transition phenomena to both the free flow and the wide moving jams. Therefore, this kind of "quasi synchronized flow state" hasn't formed an individual traffic phase, and the VDE-I model can only be considered as an intermediate model between the two-phase and the three-phase traffic flow models. Essentially, it still belongs to the fundamental diagram approach, because only the free flow phase and jammed phase are significant in this model. However, on the other hand, it implies the possible existence of a third phase and shows us a possible way to develop the models from the two-phase framework to the three-phase framework.

After the VDE-I model we carried out further modifications and developed it into a VDE-II model, published in Ref. [59]. In the VDE-II model, we execute the velocity-difference effect by changing the deceleration extent instead of the randomization

probability in the randomization process. This is equivalent to discretizing the classic car-following equation in Eq. (1) directly and representing it with a cellular automaton model. Furthermore, we introduced the slow-to-start effect into this model in order to induce the spontaneous emergence of the wide moving jams, namely, the so-called pinch effect in the three-phase traffic theory.

It is worth introducing the velocity-updating rules of the VDE-II model here. The parallel velocity-updating rules are briefly summarized as the following two steps:

1. Accelerating and braking:

$$v_n(t+1) = \min(v_n(t) + a, v_{\max}, d_n(t)) \tag{2}$$

2. Randomization with probability $p_n(t+1)$:

$$v_n(t+1) \to \max(v_n(t+1) - \Delta v, 0).$$

Here $v_n(t)$ is the velocity of vehicle n at time t (vehicle $n-1$ precedes vehicle n); d_n is the distance from the head of vehicle n to the tail of vehicle $n-1$. Let $t_{st,n}$ denote the stop time of vehicle n ($t_{st,n} = m$ means vehicle n has been stopping for m time steps currently) and t_c denote the time threshold of slow-to-start effect [56,57,59,60], the randomization probability $p_n(t+1)$ and the deceleration extent Δv are determined by the following formulations:

$$p_n(t+1) = \begin{cases} p_0 & \text{when} \quad t_{st,n} \geq t_c \\ p_d & \text{when} \quad t_{st,n} < t_c \end{cases} \tag{3}$$

$$\Delta v = \begin{cases} a & \text{when} \quad t_{st,n} \geq t_c \\ \left.\begin{matrix} b_- & \text{if } (v_n(t) < v_{n-1}(t)) \\ b_0 & \text{if } (v_n(t) = v_{n-1}(t)) \\ b_+ & \text{if } (v_n(t) > v_{n-1}(t)) \end{matrix}\right\} & \text{when} \quad t_{st,n} < t_c. \end{cases} \tag{4}$$

The rank of the acceleration and deceleration parameters above are usually required as $b_+ \geq a \geq b_-$. It's the adequate and necessary condition for the model to simulate the synchronized flow. When this condition is satisfied, the velocity-adaptation mechanics are automatically taken into account.

With these modifications, the VDE-II model shows characteristics much more consistent with the three-phase traffic theory than the previous VDE-I model. In the VDE-II model, three traffic phases are clearly distinguished, and the phase transitions among them occur with probabilities under proper density scales. This model can successfully reproduce the synchronized flow phase and the spontaneous discontinuous $S \to J$ transition, as well as the corresponding congested patterns induced by the bottleneck. However, the $F \to S$ transition in this model is not first-order but continuous. This means under any fixed vehicle densities, synchronized flow cannot spontaneously occur in free flow. In Kerner's viewpoint, both the $F \to S$ transition (breakdown phenomenon) and the $S \to J$ transition (pinch effect) can spontaneously occur under some certain densities, even on a homogeneous road. In Particular, when the breakdown phenomenon occurs, a "moving synchronized flow patten" (MSP) emerges [41,43,54]. These results are still absent in the VDE-II model.

We have discussed in Ref. [59] that Eq. (4) can be seen as another mathematical formulation of the speed-adaptation effect firstly proposed by Kerner in Refs. [41,43]. Our VDE-II model can bee seen as a combination of the KKW model and the Nagel–Schreckenberg model with slow-to-start effect. The velocity-adaptation effect can produce the synchronized flow and keep it in dynamical steady states. It's the kernel of the model to simulate the three-phase traffic flow in both the KKW models and the VDE-II model. However, on the other hand, it still needs additional mechanics to produce the first-order $F \to S$ transition. Therefore, in order to supply the absence of the breakdown phenomenon and the related MSP in the VDE-II model, we continued our work and proposed an improved model in this paper.

3. The VDE-III model

In the viewpoint of physics, the VDE-II model has overlooked the fact that the interaction range of a certain vehicle should be finite. However, in the VDE-II model, each vehicle can influence the randomization process of its following vehicle even if the follower is infinitely far away. As a result, metastable states of the free flow would be easily broken by the infinite-ranged interactions between neighboring vehicles, which causes the absence of the coexisting scale of the free flow and the synchronized flow. In this paper, following Kerner's idea [42], we are going to take into account the finite interaction range between neighboring vehicles. When exceeding this range, denoted by D_n, the randomization process of the following vehicle will become weak and independent of the preceding vehicle. Following this idea, Eqs. (3) and (4) are improved into

$$p_n(t+1) = \begin{cases} p_0 & \text{when} \quad (t_{st,n} \geq t_c) \\ p_d & \text{when} \quad (t_{st,n} < t_c \,\&\, d_n \leq D_n) \\ p_s & \text{when} \quad (t_{st,n} < t_c \,\&\, d_n > D_n) \end{cases}$$

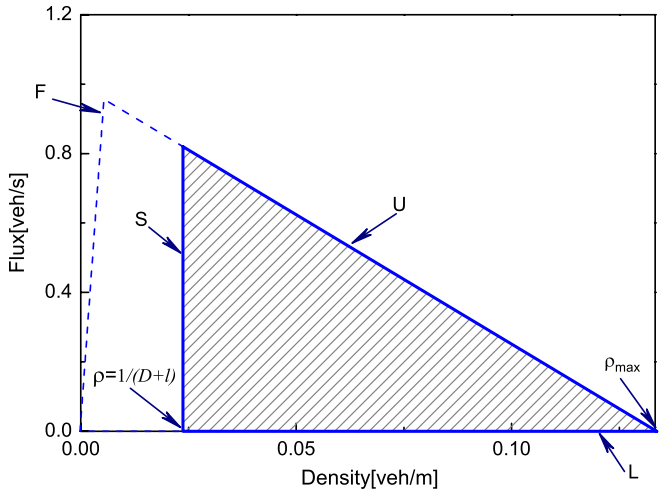

Fig. 1. (Color online) The two-dimensional region of the equilibrium states of the synchronized flow in the VDE-III model, obtained in a noiseless limit that $p_d \to 1$. The dashed line F shows the original left boundary in the VDE-II model.

$$\Delta v = \begin{cases} a & \text{when} \quad (t_{st,n} \geq t_c) \\ \left.\begin{matrix} b_- & \text{if } (v_n(t) < v_{n-1}(t)) \\ b_0 & \text{if } (v_n(t) = v_{n-1}(t)) \\ b_+ & \text{if } (v_n(t) > v_{n-1}(t)) \end{matrix}\right\} & \text{when} \quad \begin{pmatrix} t_{st,n} < t_c \\ \& \quad d_n \leq D_n \end{pmatrix} \\ b_s & \text{when} \quad \begin{pmatrix} t_{st,n} < t_c \\ \& \quad d_n > D_n \end{pmatrix}. \end{cases}$$

Here p_s and b_s are relatively smaller values. The parameters are selected as $t_c = 6, v_{\max} = 25, p_d = 0.18, p_0 = 0.5, p_s = 0.08$, $a = 2, b_- = b_s = 1, b_0 = 2, b_+ = 5$. The spatial and temporal units are selected as 1.5 m and 1 s respectively, and D_n is simplified as a constant $D = 23$.

It should be noted that a similar idea has also been presented in Kener's models [41,43]. In the KKW series models, the interaction range D_n is defined as a "synchronization distance" $D_n(\Delta x, v)$, which may be a function of the speed and headway distance. However, in this paper, we just simplify D_n to be a constant. It can be considered as one special mathematical formulation of the synchronize distance. As we are going to show in the following part, the model in this paper shows results which are reasonable enough under this special setting up of D_n. On the other hand, this constant D_n also creates small changes in the features of the synchronized flow to Kerner's models.

As well as the previous VDE-II model in Ref. [59], the VDE-III model is also equivalent to a combination of the KKW CA model [41] and the Nagel–Schreckenberg (NS) model with the slow-to-start effect [30,60] (see Eqs. (5) and (6) in Ref. [59]). Different model rules are adopted for producing different traffic phases respectively. (i) Within the interaction distance D, the updating rules of the model switch between the rules of the KKW model and the NS model with probabilities p_d (NS $\to$ KKW) and $1 - p_d$ (KKW $\to$ NS) respectively, which reproduces the synchronized flow states. (ii) At farther distance $d_n > D$, no switching between the two models occurs, the rules of the NS model with weaker noise ($p_s < p_d$) reproduces the free flow states, including the metastable states which is essentially important to the discontinuous $F \to S$ transiton. (iii) In the case $t_{st,n} \geq t_c$, the slow-to-start effect induces the spontaneous emergence of wide moving jams in the regions of synchronized flow.

By introducing the interaction range parameter D into the model, there are only short-range interactions between vehicles. As a result, the two-dimensional region covered by synchronized states has also be changed. Now we discuss the theoretical two-dimensional synchronized flow region under a noiseless limit $p_d \to 1$. In this case, the updating rules of the KKW model are adopted. As in the VDE-II model, the upper boundary U and the left boundary F are also determined by the safe speed and the maximum speed respectively, i.e.,

$$U : J_U(\rho) = v\rho = d\rho = 1 - \rho l$$

and

$$F : J_F(\rho) = \rho v_{\max}$$

where ρ is the density of vehicles, d is the distance between neighboring vehicles and l is the average length of a single vehicle (see Ref. [59]). There is still no lower boundary L in this model. However, the interaction range parameter D further restricted $d < D$, i.e.,

$$S : J(S) = \rho_{\min} = \frac{1}{D + l}$$

which defines a new left boundary F. Thus the two-dimensional region covered by the equilibrium states of the synchronized flow is restricted by the left boundary S, upper boundary U and the x axis, as shown in Fig. 1. It is apparent in the VDE-III

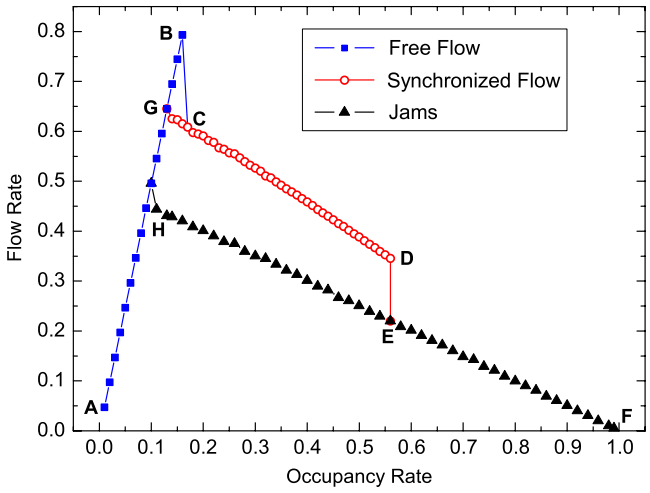

Fig. 2. (Color online) The fundamental diagram of the VDE-III model was obtained on a homogeneous circular road by starting from two different types of initial states: completely jammed states (branch AHPEF) and homogeneous states (branch ABCDEF and AGCDEF). The curves are based on simulation results within a period of 6000 time steps.

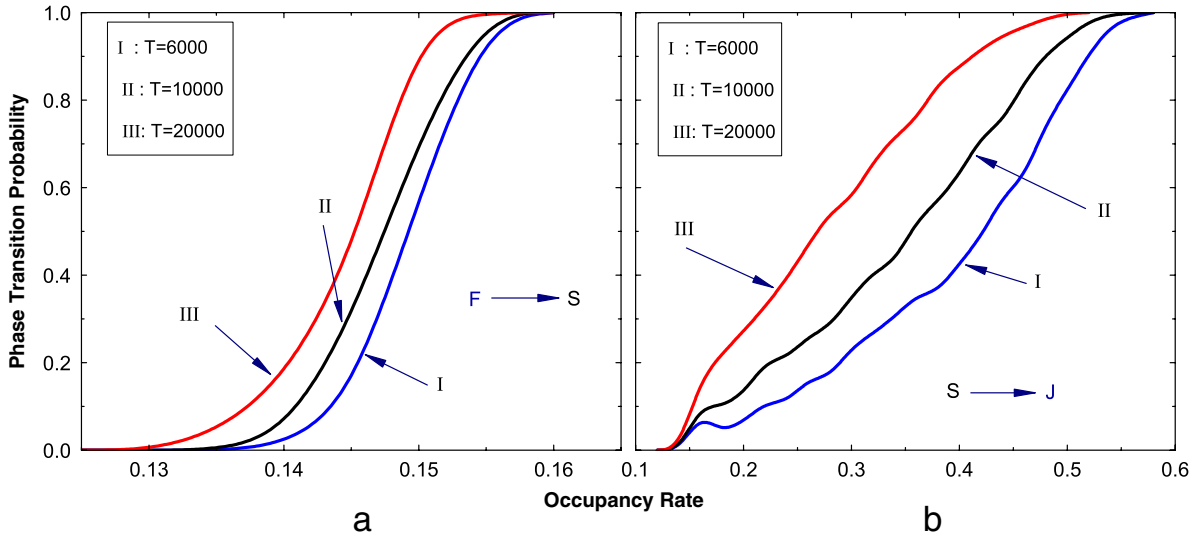

Fig. 3. (Color online) Probabilities of the spontaneous phase transitions under different densities ρ and simulation periods T. For each data point, 1000 individual runs are carried out to check whether the phase transition occurs within the given duration T under the given density ρ. The concerned probability is defined as the number of realizations in which phase transitions occur in comparison with the number of all realizations [41]. (a) $F \rightarrow S$ transition. (d) $S \rightarrow J$ transition.

model that the synchronized flow region is more limited into a scale of higher densities by comparison to the previous VDE-II model. It should also be noticed that when a similar idea was studied by Kerner [42], the boundaries of the equilibrium states induced by the synchronized distance $D_n(\Delta x, v)$ in Kerner's models were a little different.

4. Simulation results of the VDE-III model

With the VDE-III model, simulations are firstly carried out on a homogeneous circular road with the length $L = 10\,000$ cells. Fig. 2 shows the fundamental diagram of the model, in which three traffic phases and two discontinuous transitions are clearly distinguished, showing a typical double Z-characteristic structure predicted by the three-phase traffic theory [42,43]. When compared to other three-phase traffic flow models published before, the current model has a much wider hysteresis loop in flow rate scales associated with the phase transitions between the free flow and the synchronized flow. During the simulation process, the phase transitions occur with probabilities. Under the densities between point G and C in the diagram, both the free flow and the synchronized flow can exist. With probabilities, the discontinuous $F \rightarrow S$ transition occurs, corresponding to a fall of the flow rate from line GB to line GC (breakdown phenomenon). The threshold point G for the $F \rightarrow S$ transition in Fig. 2, is related to the boundary $F_{th}^{(B)}$ in the diagram of congested patterns when the on-ramp flow rate $q_{on} = 0$ on an open highway system (see Fig. 17 in Ref. [53]). In the same way, under the densities between point G and D, the discontinuous $S \rightarrow J$ transition makes the flow rate fall from line GD to line HE with probabilities (pinch effect). The corresponding phase transition probabilities are plotted in Fig. 3(a) and (b), which increase with the increase of the

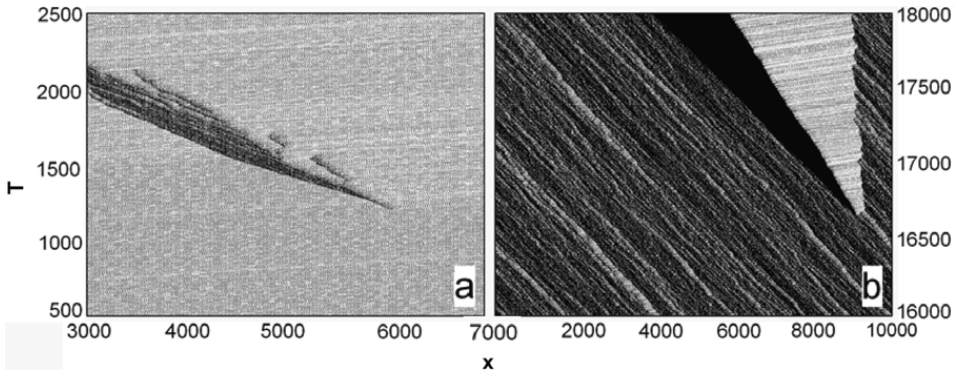

Fig. 4. Spontaneous phase transitions on a homogeneous circular road. (a) The breakdown phenomenon, synchronized flow spontaneously emerges in the free flow ($\rho = 0.145$). (b) The pinch effect, wide moving jams spontaneously emerge in the synchronized flow ($\rho = 0.45$).

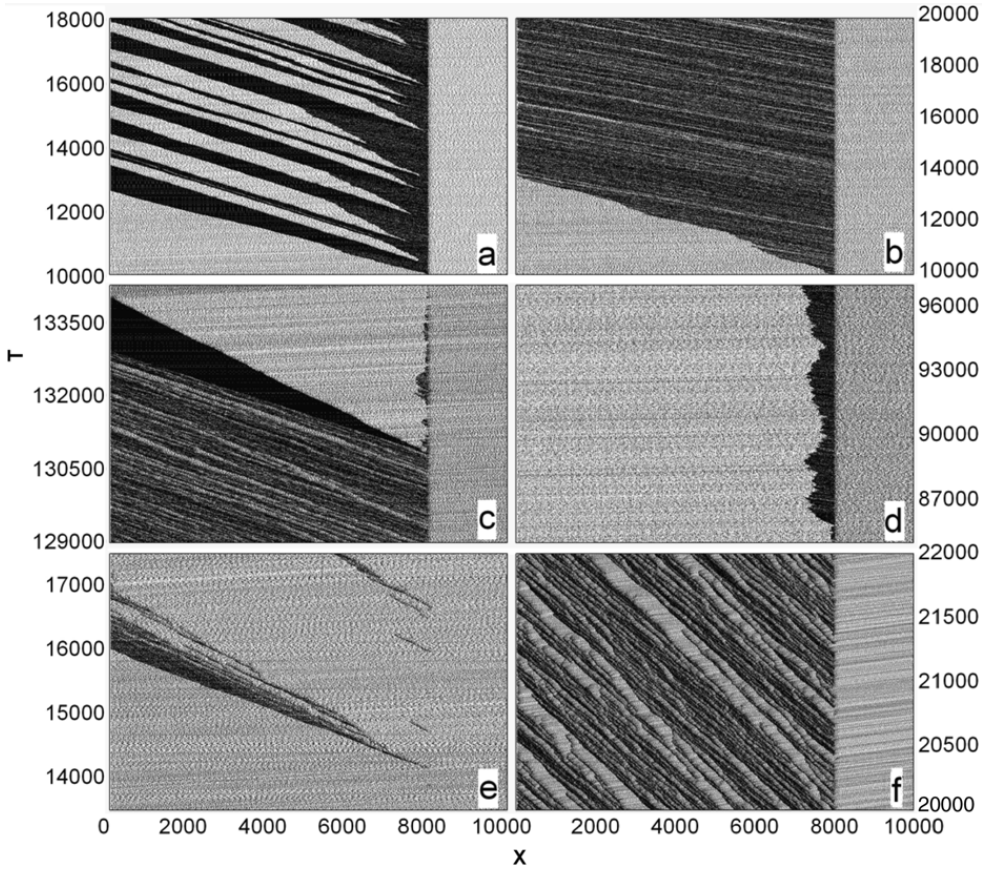

Fig. 5. (Color online) Congested patterns on an open road with the length $L = 10\,000$, having an on-ramp bottleneck at the site $x = 8000$. (a) GP ($q_{in} = 0.65$, $q_{on} = 0.30$); (b) WSP ($q_{in} = 0.6$, $q_{on} = 0.13$); (c) DGP ($q_{in} = 0.6$, $q_{on} = 0.1$); (d) LSP ($q_{in} = 0.3$, $q_{on} = 0.2$); (e) MSP ($q_{in} = 0.75$, $q_{on} = 0.005$); (f) ASP ($q_{in} = 0.6$, $q_{on} = 0.05$). Here q_{in} and q_{on} denote the flow rates on the main road and the on-ramp respectively.

density or the simulation period. Typical patterns of these phase transitions are shown on the spatial-temporal diagrams in Fig. 4(a) and (b).

The spontaneously emerged synchronized flow in Fig. 4(a), is usually realized as the "moving synchronized flow pattern" (MSP). The breakdown phenomenon with the emergence of a MSP in Kerner's prediction is well demonstrated. On the other hand, Kerner has also pointed out that the MSP can be induced by a bottleneck as well as other congested patterns. These congested patterns are plotted in Fig. 5. On a main road with a single on-ramp bottleneck, with open boundary conditions on both ends, different values of the flow rates on the main road (q_{in}) and the on-ramp (q_{on}) induces each of the six congested patterns predicted by the three-phase traffic theory. They are (a) general pattern (GP), (b) widening synchronized pattern (WSP), (c) dissolving general pattern (DGP), (d) local synchronized pattern (LSP), (e) MSP, and (f) the synchronized pattern alternation of free and synchronized flow (ASP). These results are all qualitatively the same as those found earlier in Refs. [41,43].

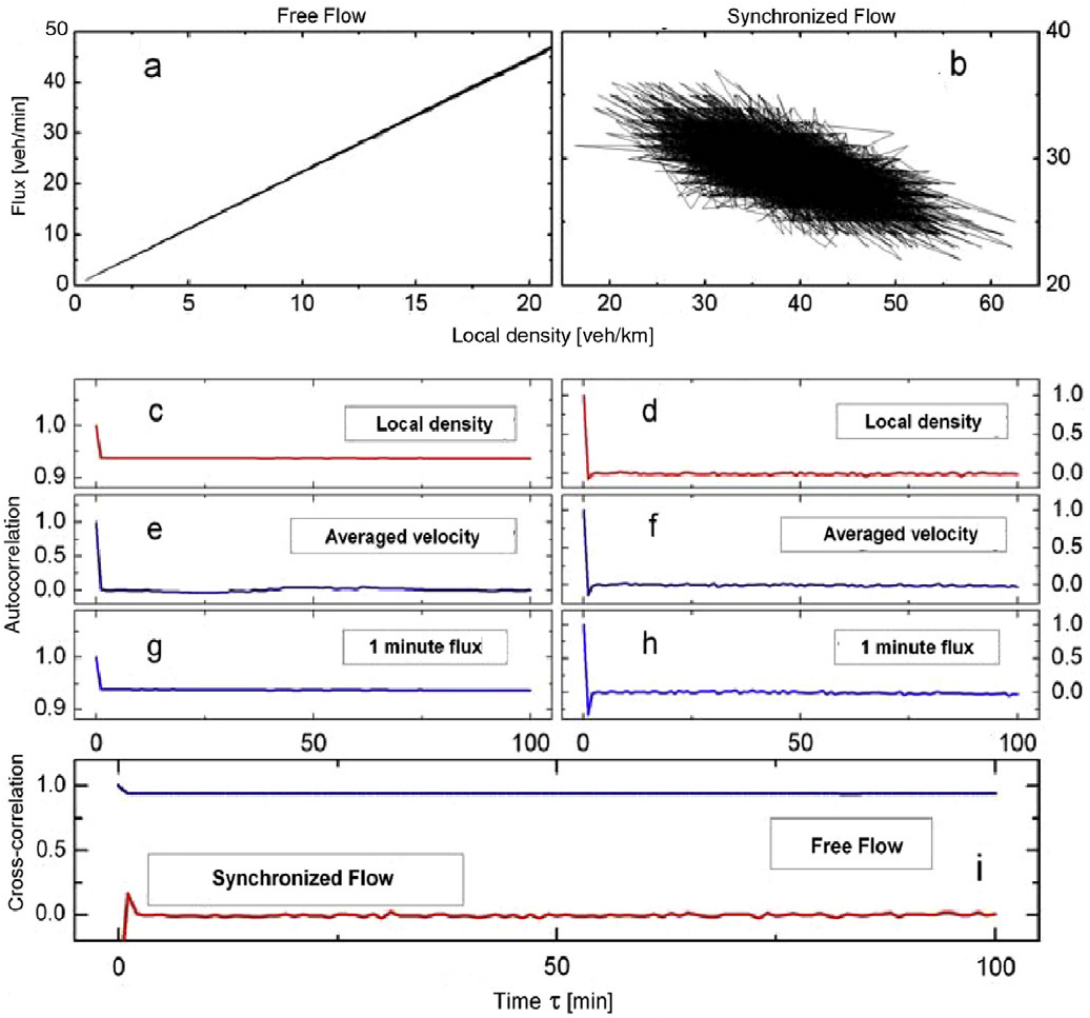

Fig. 6. (Color online) Statistics on one-minute aggregated single vehicle data obtained by loop detectors set on an open road with only one input q_{in}, varying from 0 to 1. For free flow, the road is homogeneous everywhere and q_{in} increases from 0 to 0.8 gradually; for synchronized flow, a speed-limitation of $v_{\max} = 10$ is implemented within the region (8000, 8100), and q_{in} gradually increases from 0.5 to 1.0. The road length is $L = 10000$. (a)–(b) One-minute average flow-density diagrams. (c)–(h) Autocorrelation functions for the local density, the averaged velocity and the flow flux. (i) Cross-correlation functions between the density and flow.

Now we study some statistical features of the model based on single vehicle data or one-minute aggregated single vehicle data, in order to identify the local structures of the model. Fig. 6(a) and (b) show the one-minute averaged flow-density diagrams, being well consistent with the fundamental hypothesis of the three-phase traffic theory. Fig. 6(c)–(h) show the autocorrelation functions for the local density, the averaged velocity and the flow flux. It was determined that in the free flow states, the averaged velocities are only correlated on short time scales, whereas long-ranged correlations are present in the time series of the local density as well as the flow flux. On the other hand, in synchronized flow states, all the autocorrelations are close to zero, which means no long-range correlations exist. Furthermore, Fig. 6(i) shows the cross-correlations between the density and the flux are strong for free flow while weak for synchronized flow.[1] These results are consistent with the empirical conclusions based on real measures published in Ref. [61].

It should be noted that the velocity anticipation effect is still not included in our models. This tells us that the velocity anticipation effect is not necessary for reproducing the three-phase traffic flow states. However, it does have influences on some microscopic features such as the time headway distributions. It has been discovered that the time headway distribution of traffic flow should have a cutoff on the temporal axis at a position of less than one second [37,52,61–63], which is impossible if the velocity anticipation effect was not considered. For this reason, we plotted the time headway distribution

[1] The autocorrelation function for aggregated quantities $\{x(t)\}$ and the cross-correlation function between $\{x(t)\}$ and $\{y(t)\}$ are defined as $a_x(\tau) = \frac{\langle x(t)x(t+\tau)\rangle - \langle x(t)\rangle^2}{\langle x(t)^2\rangle - \langle x(t)\rangle^2}$ and $c_{xy}(\tau) = \frac{\langle x(t)y(t+\tau)\rangle - \langle x(t)\rangle\langle y(t)\rangle}{\sqrt{\langle x(t)^2\rangle - \langle x(t)\rangle^2}\sqrt{\langle y(t)^2\rangle - \langle y(t)\rangle^2}}$. Ref. [61] has pointed out that in free flow states, for flux and density, there exist long-range autocorrelations and strong cross-correlations, which is related to the empirical daily variations in free flow. While in synchronized flow state, no long-range correlations could be found.

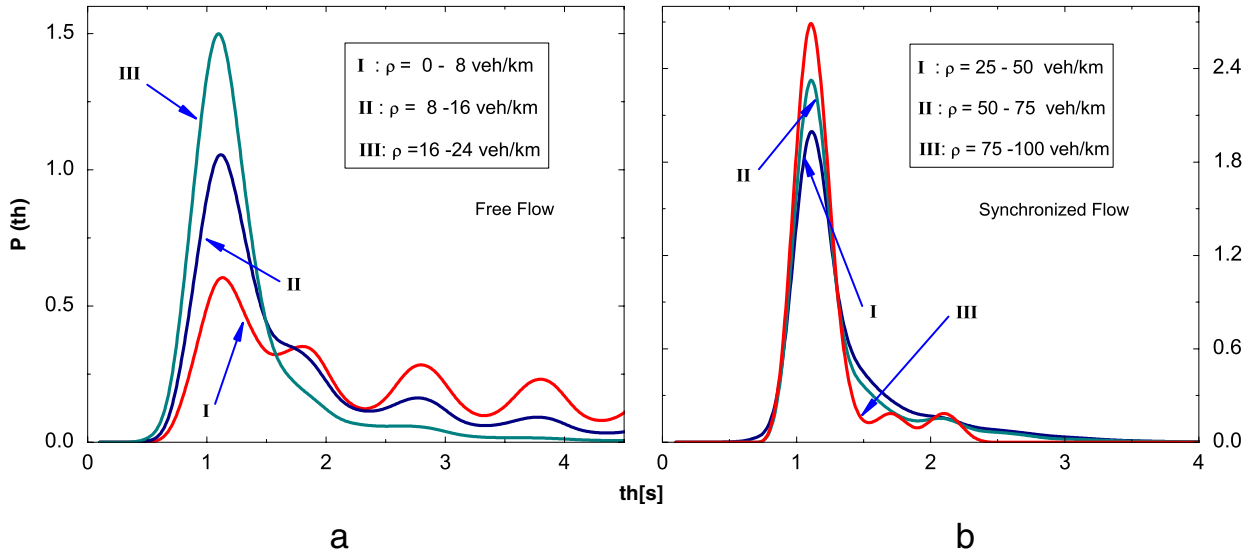

Fig. 7. (Color online) Normalized time headway distributions of the VDE-III model. (a) Free flow; (b) Synchronized flow.

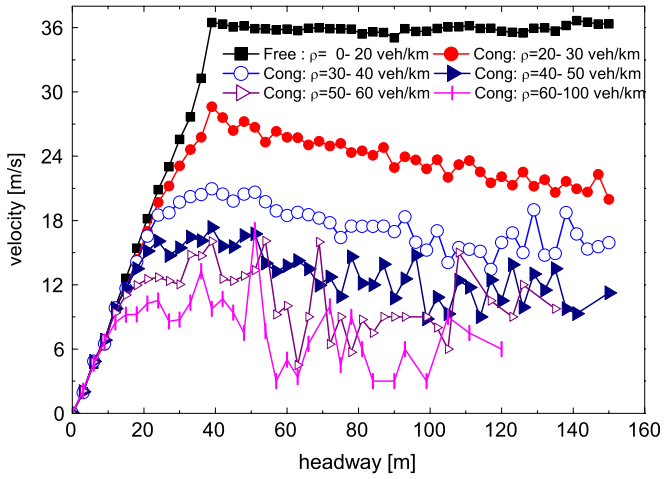

Fig. 8. (Color online) Optimal velocity (OV) functions of the VDE-III model.

of the VDE-III model in Fig. 7, with a time anticipation embedded. For this, the d_n in Eq. (2) is replaced by

$$d_{eff} = d_n + \max(0, \min(v_{n-1}(t) + a, d_{n-1}, v_{\max}) - d_{safe}).$$

The safe distance d_{safe} here is chosen as $d_{safe} = 15$, which has no qualitative influence on the simulation results above. We can see in Fig. 7 that the most important features of the time headway distribution, including the small time cutoff and the uniform positions of the maximum distributions for the free flow, are well reproduced by our model. Nevertheless, the density-dependent time headway distributions in the synchronized flow, indicated in Ref. [61,62], is still absent in our results. We surmise this might be related to multi-vehicle mixtures or multi-lane effects, and needs to be further investigated in the future.

Finally, we study the velocity-headway relations, i.e., the so-called optimal velocity (OV) functions. As shown in Fig. 8, the curves for free flow and congested flow are well separated. In free flow states, the asymptotic velocity does not depend on the density (headway), but is determined by the speed-limitation. In congested states, the asymptotic velocities are much smaller. Furthermore, the OV functions have certain distributions under large values of the headway, which makes it much better than most of the previous models in the framework of the three-phase traffic theory (see Ref. [64], most of the previous three-phase traffic models do not have a distribution of the OV function under large headways). The OV functions in Fig. 8 show features that are almost unanimous to the features shown in the Figure 4 in Ref. [62], and are consistent with the empirical findings.

5. Conclusion

Based on our previous velocity-difference series models, as a further development, we restrict in the model rules the interactions between neighboring vehicles to be short-ranged. This avoids an unrealistic dynamic in the VDE-II model

that vehicles always have interactions with their neighbours even if the neighbors are infinitely faraway. As a result, the simulation results of the modified model become more consistent with the predictions of the three-phase traffic theory. The major improvements are: (1) The improved model reproduces the discontinuous transition from the free flow to the synchronized flow, together with the breakdown phenomenon and the moving synchronized flow pattern, which are all absent in the previous two VDE models but have been observed by Kerner and predicted in his three-phase traffic theory. (2) The improved model shows better microscopic characteristics than the previous VDE models. It simulates the correlation functions identical to the empirical results not only for synchronized flow states, but also for free flow states. The result implies that the free flow is not as trivial as we thought before. (3) The improved model reproduces most features of the empirical time-headway distributions. On the other hand, the reproduced OV functions are highly consistent with the empirical results, which is an obvious improvement when compared to previous models.

Besides the improvements in describing traffic characteristics, by proposing the VDE-III model in this paper, we finally established a gradual transformation within a model series from the framework of the traditional "fundamental diagram approach" to the three-phase traffic theory. From the VDE-I model to the VDE-III model, the transformation process of the model rules and the simulation results induced by these rules may be helpful for our understanding of the essential dynamics of the traffic flow. We learnt from this trip that: (1) When reproducing the synchronized flow, it may be important in the future to determine the correct interaction mechanics between the neighboring vehicles under certain densities, such as the velocity-difference effect, for example. (2) The slow-to-start effect shows a valuable suggestion on how wide moving jams spontaneously emerge in some less congested regimes, like in the synchronized flow. (3) The short-range limitation on the interactions between neighboring vehicles makes the exitance of metastable states of free flow possible and shows us a discontinuous transition to congested traffic.

We have also leant that the parameter of the interaction range between vehicles could be effective enough under the very simplest form. The constant parameter shows different features to the velocity-related parameters in Kerner's models. As for the velocity anticipation effect, it shows less importance in influencing the macroscopic features of the outputs but is quite important to the microscopic structures.

Acknowledgements

This work is funded by the National Basic Research Program of China (No. 2006CB705500), the National Natural Science Foundation of China (Grant Nos. 60744003, 10635040, 10532060, 10872194), and the Specialized Research Fund for the Doctoral Program of Higher Education of China.

References

[1] D. Helbing, Traffic and related self-driven many particle systems, Rev. Modern Phys. 73 (2001) 1067–1141.
[2] D. Chowdhury, L. Santen, A. Schadschneider, Statistical physics of vehicular traffic and some related systems, Phys. Rep. 329 (2000) 199–329.
[3] T. Nagatani, The physics of traffic jams, Rep. Prog. Phys. 65 (2002) 1331–1386.
[4] A. Schadschneider, in: M. Schreckenberg, D. Wolf (Eds.), Traffic and Granular Flow 97, Springer, Singapore, 1998.
[5] F.L. Hall, B.L. Allen, M.A. Gunter, Empirical analysis of freeway flow-density relationships, Transp. Res. A 20 (2002) 197–210.
[6] R. Mahnke, J. Kaupuzs, I. Lubanshevsky, Probabilistic description of traffic flow, Phys. Rep. 408 (2005) 1–130.
[7] H.Y. Lee, H. Lee, D. Kim, Phase diagram of congested traffic flow: An empirical study, Phys. Rev. E 62 (2000) 4737–4741.
[8] M. Treiber, A. Hennecke, D. Helbing, Congested traffic states in empirical observations and microscopic simulations, Phys. Rev. E 62 (2000) 1805–1824.
[9] M. Schoenhof, D. Helbing, Empirical features of congested traffic states and their implications for traffic modeling, Transp. Sci. 41 (2007) 135–166.
[10] K. Nagel, D.E. Wolf, P. Wagner, P. Simon, Two-lane traffic rules for cellular automata: A systematic approach, Phys. Rev. E 58 (1998) 1425–1437.
[11] P.I. Richards, Shock waves on the highway, Oper. Res. 4 (1956) 42–51.
[12] H.J. Payne, Freflo: A macroscopic simulation model for freeway traffic, Transp. Res. Rec. 722 (1979) 68–77.
[13] C.F. Daganzo, Requiem for second-order fluid approximation of traffic flow, Transp. Res. B 29 (1995) 277–286.
[14] M.J. Lighthill, G.B. Whitham, On kinematic waves: Ii. a theory of traffic flow on long crowed roads, Proc. Roy. Soc. Ser. A 229 (1955) 317–345.
[15] P.I. Richards, Shock waves on the highway, Oper. Res. 4 (1956) 42–51.
[16] H.J. Payne, Models of freeway traffic and control, in: G.A. Bekey (Ed.), in: Mathematical Models of Public Systems, vol. 1, Simulation Council, La Jolla, 1971, pp. 51–61.
[17] H.J. Payne, Freflo: A macroscopic simulation model for freeway traffic, Transp. Res. Rec. 722 (1979) 68–77.
[18] C.F. Daganzo, Requiem for second-order fluid approximation of traffic flow, Transp. Res. B 29 (1995) 277–286.
[19] R. Jiang, Q.S. Wu, Z.J. Zhu, A new continuum model for traffic flow and numerical tests, Transp. Res. B 36 (2002) 405–419.
[20] R. Jiang, Q.S. Wu, Z.J. Zhu, A new dynamics model for traffic flow, Chin. Sci. Bull. 46 (2001) 345–349.
[21] I. Prigogine, R. Herman, Kinetic Theory of Vehicular Traffic, American Elsevier, New York, 1971.
[22] S.L. Paveri-Fontana, On Boltzmann-like treatments for traffic flow. A critical review of the basic model and an alternative proposal for dilute traffic analysis, Tranp. Res. 9 (1975) 225–235.
[23] D. Helbing, Derivation and empirical validation of a refined traffic flow model, Physica A 233 (1996) 253–282.
[24] M. Treiber, A. Hennecke, D. Helbing, Derivation, properties, and simulation of a gas-kinetic based, nonlocal traffic model, Phys. Rev. E 59 (1999) 239–253.
[25] A. Reuschel, Oesterreichisches Ingenieur-Archir 4 (1950) 193–215.
[26] L.A. Pipes, J. Appl. Phys. 24 (1953) 274–287.
[27] M. Cremer, J. Ludwig, A fast simulation model for traffic flow on the basis of boolean operations, J. Math. Comput. Simul. 28 (1986) 297–303.
[28] S. Wolfram, Statistical mechanics of cellular automata, Rev. Modern Phys. 55 (1983) 601–644.
[29] O. Biham, A.A. Middleton, D.A. Levine, Self-organization and a dynamical transition in traffic flow models, Phys. Rev. A 46 (1992) R6124–R6127.
[30] K. Nagel, M. Schreckenberg, J. Physique I 2 (1992) 2221.
[31] D. Helbing, Rev. Modern Phys. 73 (2001) 1067–1141.
[32] B.S. Kerner, The Physics of Traffic, Springer, Berlin, New York, 2004.
[33] B.S. Kerner, Transp. Res. Rec. 1678 (1999) 160–167.
[34] B.S. Kerner, H. Rehborn, M. Aleksic, A. Haug, Transp. Res. C 12 (2004) 369–400.

[35] B.S. Kerner, H. Rehborn, A. Haug, I. Maiwald-Hiller, Traffic Eng. Control 46 (10) (2005) 380–385.
[36] B.S. Kerner, S.L. Klenov, A. Hiller, H. Rehborn, Phys. Rev. E 73 (2006) 046107.
[37] B.S. Kerner, S.L. Klenov, A. Hiller, J. Phys. A: Math. Gen. 39 (2006) 2001–2020.
[38] B.S. Kerner, H. Rehborn, Phys. Rev. Lett. 79 (1997) 4030.
[39] B.S. Kerner, H. Rehborn, Phys. Rev. E 53 (1996) R1297.
[40] B.S. Kerner, H. Rehborn, Phys. Rev. E 53 (1996) R4275.
[41] B.S. Kerner, S.L. Klenov, D.E. Wolf, J. Phys. A 35 (2002) 9971.
[42] B.S. Kerner, S.L. Klenov, J. Phys. A 39 (2006) 1775.
[43] B.S. Kerner, S.L. Klenov, Phys. Rev. E 68 (2003) 036130.
[44] B.S. Kerner, Phys. Rev. Lett. 81 (1998) 3797.
[45] B.S. Kerner, Phys. Rev. E 65 (2002) 046138.
[46] K. Nishinari, M. Treiber, D. Helbing, Phys. Rev. E 68 (2003) 067101.
[47] D. Helbing, D. Batic, M. Schoenhof, M. Treiber, Physica A 303 (2002) 251–260.
[48] M. Treiber, D. Helbing, J. Phys. A 32 (1999) L17–L23.
[49] D. Helbing, A. Hennecke, M. Treiber, Phys. Rev. Lett. 82 (1999) 4360.
[50] H.Y. Lee, H.W. Lee, D. Kim, Phys. Rev. Lett. 81 (1998) 1130.
[51] H.Y. Lee, H.W. Lee, D. Kim, Phys. Rev. E 59 (1999) 5101.
[52] W. Knospe, L. Santen, A. Schadschneider, M. Schreckenberg, Phys. Rev. E 65 (2002) 056133.
[53] B.S. Kerner, Physica A 333 (2004) 379.
[54] B.S. Kerner, S.L. Klenov, J. Phys. A 35 (2002) L31.
[55] H.K. Lee, R. Barlovic, M. Schreckenberg, D. Kim, Phys. Rev. Lett. 92 (2004) 238702.
[56] R. Jiang, Q.S. Wu, J. Phys. A 36 (2003) 381.
[57] R. Jiang, Q.S. Wu, European Phys. J. B 46 (2005) 581.
[58] S.X. Hu, K. Gao, B.H. Wang, Y.F. Lu, C.J. Fu, Physica A 386, 397–406.
[59] K. Gao, R. Jiang, S.X. Hu, B.H. Wang, Q.S. Wu, Phys. Rev. E 76 (2007) 026105.
[60] R. Barlovic, L. Santen, A. Schadschneider, M. Schreckenberg, Eur.Phys.J.B 5 (1998) 793.
[61] L. Neubert, L. Santen, A. Schadschneider, M. Schreckenberg, Phys. Rev. E 60 (1999) 6480.
[62] W. Knospe, L. Santen, A. Schadschneider, M. Schreckenberg, Phys. Rev. E 70 (2004) 016115.
[63] B. Tilch, D. Helbing, in: D. Helbing, H.J. Herrmann, M. Schreckenberg, D.E. Wolf (Eds.), Traffic and Granular Flow '99, Springer, Berlin, 2000.
[64] Y.M. Yuan, R. Jiang, Q.S. Wu, Characteristics analysis and empirical test of three cellular automaton models for synchronized flow, 2006.